CONCRETE LIBRARY OF JSCE NO. 36, DECEMBER 2000

EVALUATION OF DEGREE OF ASR DETERIORATION IN CONCRETE AND ANALYSIS OF PORE SOLUTIONS

(Translation from Proceeding of JSCE ,No.641/V-46,February 2000)


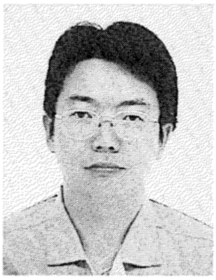
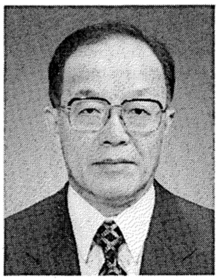

Hiroyuki KAGIMOTO Michio SATO Mitsunori KAWAMURA

This study aims at investigating the influence of local environmental conditions on the degree of damage in existing ASR-damaged concrete structures and proposing a method for predicting the future progress of ASR damage on the basis of the resulting data. ASR damage was found to proceed rapidly after the number of annual freezing-thawing cycles increased as a result of climate changes. It was also found that the degree of deterioration in concrete depends on local conditions, such as temperature, humidity, and the supply of water from the outside. A combination of the alkalinity of extracted pore solution and residual expansion of concrete cores taken from the structures as measured by the NBRI test provides a useful means of predicting the future progress of ASR damage in concrete structures.

Key Words : *ASR, environment, evaluation of deterioration, pore solution, prediction of deterioration, NBRI test*

Hiroyuki Kagimoto is a civil engineer in Civil Engineering & Architecture Department at Electric Power Development Co., Ltd. He obtained his M.S. degree from Kyoto University in 1987. His research interests relate to the alkali-silica reaction and dam concrete with fly ash. He is a member of JSCE.

Michio Sato is a civil engineer in Chigasaki R&D center at Electric Power Development Co., Ltd. He obtained his M.S. degree from Tohoku University in 1992. His research interests relate to the concrete durability. He is a member of JSCE.

Mitsunori Kawamura is a professor in the Department of Civil Engineering at Kanazawa University. He has been active in cement and concrete research for 30 years. His research interests include the alkali-silica reaction, concrete durability, and the microstructure of cement-based materials. He is a fellow of the JSCE.

1. INTRODUCTION

Many studies concerning ASR have been carried out. From these studies, the mechanism of ASR, as well as the factors influencing it, have been understood. It is well known that ASR is a chemical reaction between the pore solution in concrete and reactive aggregates. It is accelerated by alkalis supplied by cement, aggregates, and chemical admixtures. Temperature and humidity combine to affect ASR damage in concrete. In addition, it has been pointed out that the degree of damage to a concrete structure due to ASR varies widely depending on the environment. In the structures influenced by sea water and snow melting agents, we know that NaCl and melting agents supplied externally accelerate ASR[1]. However, there have been few studies that look at the progress of deterioration in reactive aggregate-containing concretes under different environments over long periods. Indeed, most studies concerning ASR have been carried out in laboratories, and only a few have dealt with concrete structures in natural environments.

Meanwhile, from a maintenance perspective, it is important not only to predict the actual progress of ASR, but also to find a rational method of predicting it. The progress of ASR is influenced by the concentration of alkalis in the pore solution and by the reactive components of aggregates. The former have been studied by discussing the mechanism of ASR in terms of the ion concentrations in the pore solution[2][3], but they have been carried out only for cement pastes and mortars in the laboratory; none have dealt with ions in the pore solution of concrete structures in natural environments. Regarding the aggregates, we have found no rational proposal for judging whether concrete contains reactive components or not. Thus, most studies concerning ASR have been laboratory investigations, and few have dealt with concrete structures in natural environments. In this study, we investigate concrete retaining walls which have been severely damaged by ASR in natural environments. The purposes of the study are as follows:

(1) Evaluation of degree of deterioration under various environmental conditions
We evaluate and reveal the effect of environmental conditions (temperature, humidity, etc) on the degree of ASR damage.

(2) Analysis and evaluation of pore solution in order to predict progress of ASR damage in concrete structure.
ASR is a chemical reaction between alkalis in the pore solution and reactive components in the aggregates. We discuss the possibility of predicting the progress of ASR deterioration by combining information on the concentration of alkalis in the pore solution with a judgment on the existence of reactive components in concrete cores.

2. OVERVIEW OF OUR STUDY

2.1 Structures investigated

The structures investigated in this study are concrete retaining walls constructed as part of a new "rubber" weir. Generally, concrete weirs installed in the upper reaches of rivers suffer from severe deterioration as a result of impact, abrasion, and wear caused by earth, sand, and rocks. We constructed a new design of rubber weir in 1982 in order to overcome these problems by raising and lowering it. The rubber weir consists of two concrete retaining walls, each 10m high, 14m wide width, and a gradient of 1:05. An air-inflated weir of abrasion-proof rubber was anchored to the retaining walls on both banks, and was designed to be deflated when the water depth reached 5.3m and raised when it was at 0.2m by an automatic water level sensor(Fig.1,2). A concrete bracing wall was constructed behind the concrete retaining wall on the right bank. At the left bank, the retaining wall was back-filled with soil. When this study began in 1996, fourteen years had elapsed since the structure was built and severe deterioration, primarily caused by ASR, was observed.

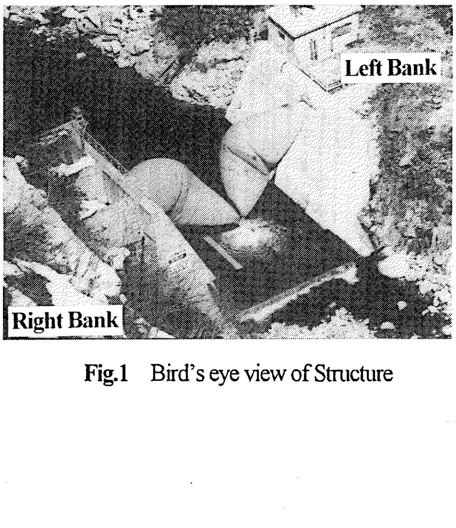

Fig.1 Bird's eye view of Structure

2.2 Summary of pore solution extraction tests

ASR is one type of deterioration caused by chemical reactions occurring within the concrete. This chemical reaction takes place between reactive components in the aggregate and pore solution. In investigating ASR deterioration, it is essential to evaluate the chemical constitutions of the pore solution, which are primarily sodium hydroxide and potassium hydroxide. Pore solution

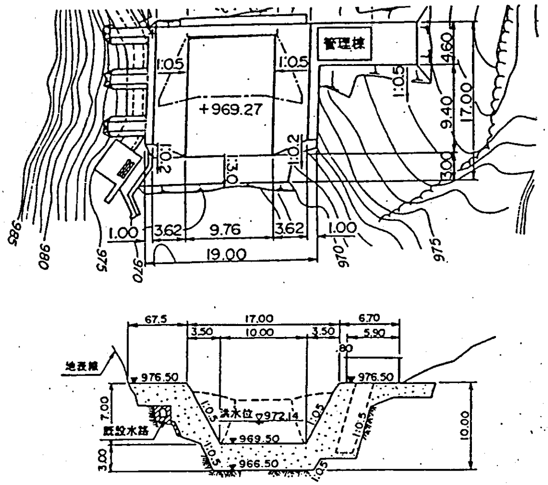

Fig.2 Plan and cross section of dam

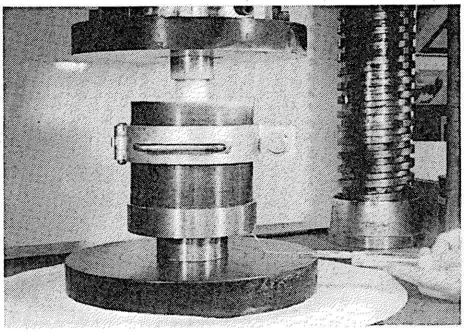

Fig.3 High-pressure apparatus for extracting pore solution

can be extracted from concrete cores in high-pressure apparatus[2]. The analysis of pore solution for evaluating ASR deterioration generally entails measuring Na^+,K^+,Ca^{2+}, and OH^- ion concentrations. Positive ions ($\Sigma+$) and negative ions ($\Sigma-$) are always balanced in the pore solution, so we can verify the analysis by determining whether the difference between $\Sigma+$ and $\Sigma-$ is less than 10% or not.

$$\Sigma- = [OH^-]$$
$$\Sigma+ = [Na^+]+[K^+]+2[Ca^{2+}]$$

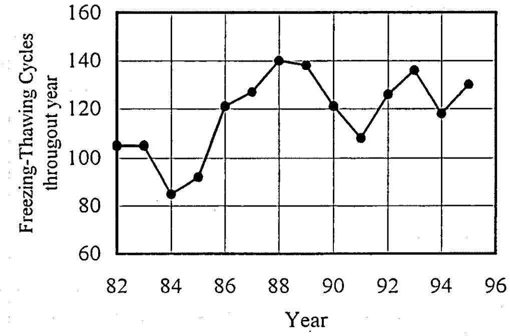

Fig.4 Changes in freezing-thawing cycles by each year

Generally, as compared with $[Na^+]$ $[K^+]$, the $[Ca^{2+}]$ ion concentration is about 1/10-1/100, so we can think of the alkali ion concentration as $[Na^+]+[K^+]$ ($\fallingdotseq [OH^-]$).

$$\text{Alkali ion concentration} \fallingdotseq [Na^+]+[K^+] \quad (\fallingdotseq [OH^-])$$

As noted in Section 1, one of the purposes of this study is to predict the future progress of deterioration in ASR damaged structures by comparing the chemical constitution of the pore solutions and the presence of residual reactive components. However, as there are no data available on the chemical constitution of pore solutions in cement paste or mortar where various water/cement ratios were used, we first had to confirm the effect of water/cement ratio by carrying out a pore solution analysis using cement paste and mortar specimens. Following this test, we extracted pore solution from concrete cores taken from the actual structure, and analyzed these solutions. To extract the pore solutions, we connected a high-pressure apparatus to a 200-t universal test unit, and repetitively applied and released loads up to approximately 600 kN in incremental steps (Fig.3). The extracted pore solutions were immediately diluted with 100 to 200 parts of water. Then Na^+, K^+, and Ca^{2+} ion concentrations were measured by the ICP method and OH^- by titration against hydrochloric acid to the phenolphthalein end point. To prevent loss of alkalis from the concrete cores, cores extracted on site were immediately sealed in vinyl bags. Later, in the laboratory, from the central portions of the 96mm-diameter original cores, cores measuring 46 mm in diameter and 100 mm in length were drilled. Immediately after drilling, 2 to 3 ml of pore solution was extracted from these smaller cores for analisis.

3. FIELD STUDY OF ASR-DETERIORATED STRUCTURE AND EVALUATION OF DEGREE OF DETERIORATION

3.1 Local environmental conditions

a) Climate conditions in the area

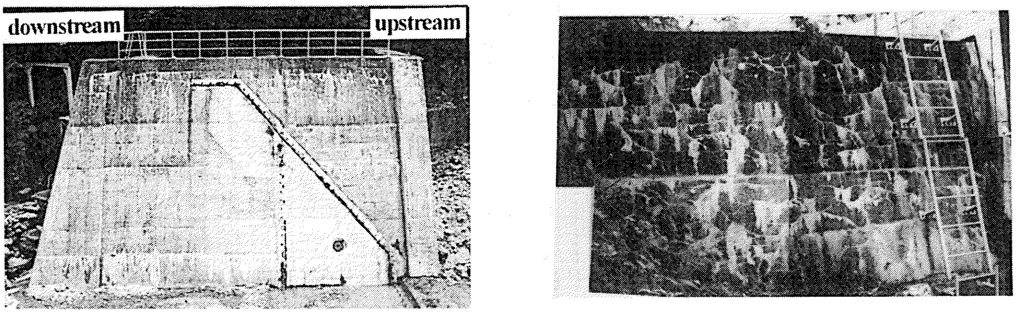

(a) right bank (b) Rear face of retaining wall

Fig.5 Appearance of surface of structure

Weather records for the rubber weir and at a weather station located some 8 km southwest of the rubber weir indicate that the maximum air temperature in summer exceeded 35°C and the minimum temperature in winter fell below -15°C in some years. It was also recorded that the area experienced heavy snowfall. Fig.4 shows the variation in the number of freezing-thawing cycles (when the day's minimum temperature fell below freezing point and the maximum temperature rose above freezing point) over the period of 14 years from 1982, when the rubber weir was completed, to 1995. The figure shows that the number varied around 100 per annum up to 1985, but reached 140 in 1988 and has settled at around 130 per annum in recent times.

b) Environmental conditions of concrete retaining wall

While the concrete retaining wall on the right bank of the rubber weir was not exposed to much solar radiation during the year because a steep cliff overhangs the bank, the left bank was strongly affected by isolation. Observations of water level indicate that the rubber weir is typically lowered during the freshet period from early summer to autumn to keep the water level low, while it is elevated in winter to maintain the water at a higher level. This means that the lower section of the concrete retaining walls on the upstream side are permanently immersed in water during the winter and are not subjected to the freezing-thawing process. It can, however, be inferred that those sections on the downstream side that are exposed to the atmosphere are subject to severe cycling during the winter.

As indicated in Fig.5 (a), the surface of the concrete retaining wall that was covered with the rubber weir (the trapezoidal section at the center) was not directly exposed to the external environment and thus exhibited a totally different deterioration pattern. Additional characteristics of the exposure environment are described below.

●Right bank

The rear face of the retaining wall and the bracing concrete portions were in a permanently damp condition, being covered by thick plant growth including ferns. (Fig.5 (b))

●Left bank

Most of the rear face of the retaining wall was back-filled with soil and was thus in a damp condition. A machine room at the first basement level of the administration building was maintained inside in a relatively dry condition. (Fig.1)

3.2 Results of investigation and evaluation of degree of deterioration

a) Aging of concrete retaining walls

Fig.6 shows the surface appearance of the retaining wall on the downstream side of the right bank. These photographs show that the progress of deterioration between 1989 and 1992 was considerable. In particular, a comparison of the overall appearance of the concrete body in 1989 with that in 1992 indicates the following: Whereas no trace of gel was observed on the surface in 1986, a significant volume was extruding from many cracks the concrete in 1992. It is possible to explain the changes in appearance of the

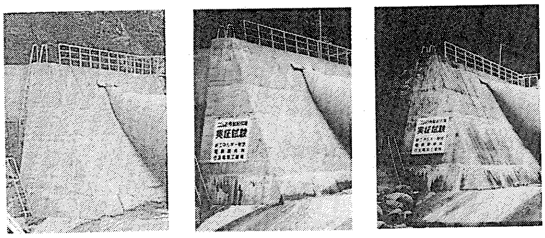

1986 1989 1992

Fig.6 Changes in appearance of structure during period 1986 to 1992 concrete body as follows. It appears that many cracks were caused by ASR in the concrete retaining walls from an early stage after construction. As shown in Fig.4, the number of freezing-thawing cycles drastically increased after 1987. This increase in the number of cycles in 1988 is found to correspond to a drastic aggravation of the concrete condition. The infiltration of water through these cracks accelerated the absorption of water by gels which transform to sols. Accordingly, many factors were involved in the progress of ASR deterioration in the walls, including the progress of cracking caused by freezing-thawing cycles. It is presumed that deterioration must also be promoted by the combined effect of these factors.

b) Density of cracks on concrete retaining wall surface

Visual observations of the condition of the retaining wall surfaces indicated a notable number of hexagonal-pattern cracks at the thin top portion of the retaining wall, where the temperature rise was great. This indicates an advanced stage of ASR deterioration. It was also noted that the density of these cracks was considerable. Comparing the surface of the concrete body on the right and left bank, it was found that the crack density on the left bank, which was exposed to longer periods of solar radiation, was greater than that on the right bank.

Further, the downstream portion which had been severely damaged by freezing-thawing cycles exhibited a greater number of cracks than the bottom steps on the upstream side, which were immersed in water during the winter. There were also very few cracks in the portion covered by the rubber weir (light portion at the center in the photograph) and these cracks were minute, because this portion was completely protected from freezing damage (Fig.5(a)). In order to evaluate differences in the degree of local deterioration quantitatively, we calculated the crack density (Table.1). Here, the crack density refers to the value obtained by dividing the number of cracks that intersect traverse lines drawn at 10cm intervals (evaluated within an area of 1.2 m × 1.2m) by the total extension of the traverse lines. This quantitative evaluation revealed the following:

1. Crack density is greater on the left bank (3.05: upstream), where exposure to solar radiation is greater, than on the right bank (1.50: upstream);
2. Crack density is greater at the top steps, where the temperature rise was estimated to be great due to the smaller cross-sectional area (2.96: upstream; 4.45: downstream), than at the bottom steps (1.60: upstream; 3.00: downstream);
3. Crack density is greater in areas maintained in a damp condition due to thick foliage and plants (6.79: rear face of the right bank) than elsewhere; and
4. Crack density is greater at the bottom steps of the downstream side(3.00) where complex damage by freezing was observed than at the bottom steps on the upstream side (1.60).
5. The rubber weir anchorage area, which was protected from solar radiation and water, exhibited no signs of conspicuous cracking, although a few minute cracks were observed.

These observations lead to the following conclusions:

The degree of deterioration caused by ASR varies locally, depending on environmental conditions including temperature, humidity, freezing-thawing damage, and their combined effects. Crack generation at the concrete surface can be substantially reduced by reducing temperature and humidity changes and by restricting the water content. It is inferred, from the area covered by the rubber weir, that repeated freezing-thawing cycles and wetting-drying cycles are considerably alleviated by the rubber covering over the concrete walls, resulting in great differences in degree of deterioration within the same structure. Thus, differences in the local environmental have a significant effect on the deterioration caused by ASR.

Table 1 Crack density on concrete surface

			crack density (n/L)			Remarks
			left bank	right bank	average	
FRONT	upstream	upper part	3.55	2.36	2.96	
		lower part	2.55	0.64	1.60	
		average	3.05	1.50	2.28	
	downstream	upper part	3.95	4.95	4.45	right bank: high humidity
		lower part	3.32	2.68	3.00	
		average	3.64	3.82	3.73	
rubber part			0.00	0.00	0.00	hair crack
rear part		average	—	6.79	—	high humidity

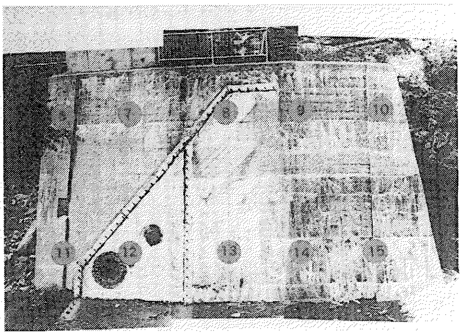

Fig.7 Location of Schmidt hammer tests

c) Surface strength of concrete retaining walls

A Schmidt rebound hammer was used to estimate the surface strength of the retaining wall surfaces. Fig.7 shows the points tested with the Schmidt rebound hammer. Table2 gives the results obtained. These reveal the following :

(1) Strength is slightly greater at the top step (left bank:26.3N/mm^2 ; right bank:27.4N/mm^2) than at the bottom step (left bank: 29.9N/mm^2 ; right bank:31.2N/mm^2) where there is more radiation. And the surface strength on the left bank is slightly below that at the right bank because of the greater effect of solar radiation.

(2) Strength at the rubber weir anchorage (34.2 - 36.8 N/mm^2), where solar radiation and water content were cut off, is markedly greater than in other areas.

Table 2 Result of Schmidt hammer tests

point	No.	test area	environment	strength (N/mm^2)	Remarks
LEFT SIDE	6	upper part	open	20.2	Average ・upper part = 26.3 ・open part = 24.4 ・rubber part = 34.2
	7		〃	25.3	
	8		rubber	34.2	
	9		open	27.9	
	10		〃	24.0	
	11	lower part	open	22.8	Average ・lower part = 29.9 ・open part = 25.3 ・rubber part = 36.8
	12		rubber	36.8	
	13		〃	36.8	
	14		open	25.3	
	15		〃	27.9	
	average				28.1
RIGHT SIDE	18	upper part	open	24.0	・upper part = 27.4 ・open part = 25.6 ・rubber part = 34.2
	19		〃	26.6	
	20		rubber	34.2	
	21		open	24.0	
	22		〃	27.9	
	23	lower part	open	22.8	・lower part = 31.2 ・open part = 28.3 ・rubber part = 35.5
	24		〃	30.4	
	25		rubber	38.1	
	26		〃	33.0	
	27		open	31.7	
	average				29.3
average					28.7

These observations indicate that the degree of deterioration of ASR-damaged concrete is affected by solar radiation, and that alleviation of temperature changes and cutting the supply of water can significantly reduce the loss of strength in concrete.

d) Compressive strength and modulus of static elasticity of cores

Concrete cores (diameter: 96 mm; length: 2 m) were drilled from the left and right bank retaining walls. Table3 gives the exposure environment at the core extraction locations. The strength of the cores was compared by considering several parameters, including humidity, solar radiation, and depth from the surface. Fig.8 indicates the relationship between strength and modulus of the static elasticity of these cores. A certain degree of proportionality can be observed. The modulus of static elasticity of these cores were found to be far below[4] the calculated values indicated in the standard specifications for concrete, as stipulated by the JSCE. It is inferred that the lower modulus of static elasticity values obtained for cores extracted from the top steps than for cores extracted from the bottom steps reflects differences in the degree of cracking. Fig.9 shows the relationship between depth of core and core strength. This leads to the following findings:

Table 3 Environmental conditions at locations from which concrete cores were drilled

boring core No.		length (cm)	environment(front)		environment(rear)				sunshine			humidity(rear)		Remarks
			open	rubber	basement	ground	foliage	concrete	front	rear	side	guantity	altemation	
left bank	①	199	○				side	○	◎	−	×	○	△	※1
	②	192	○		○				◎	×	−	△	△	
	③	192	○	△		○			○	−	−	◎	△	
	④	216	○				○		◎	×	◎	○	△	※2
right bank	⑤	204	○					○	△	−	○	△	△	※3
	⑥	179	○				○		△	×	−	◎	△	
	⑦	180		○			○		×	×	−	◎	△	
	⑧	182	○					○	△	−	−	−	−	

※1 10cm between core and side surface(foliage)
※2 50cm between core and side surface
※3 10cm between core and side surface(open)

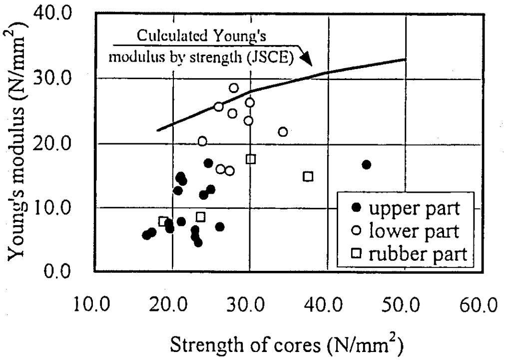

Fig.8 Relations between core strength and Young's modulus

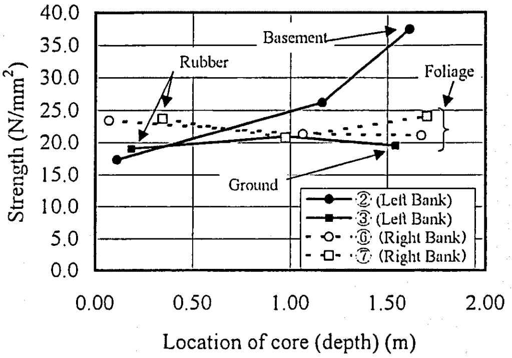

Fig.9 Strength of concrete cores(Φ96mm)

(1) Compared with the strength of cores taken from points ⑥ and ⑦ near the surface of the upper steps on the right bank, the strength of cores taken from points ② and ③ near the surface of the upper steps on the left bank is much lower due to longer exposure to solar radiation.

(2) The core strength is low at points ⑥ and ⑦ at the upper steps on the right bank and point ③ at the upper steps on the left bank, where humidity was always high due to soil backfilling and the abundance of foliage.

(3) The core strength is greater around the rear face of the upper step point ② in the machine room, which was maintained in a dry condition.

(4) The strength at the lower steps of the retaining wall was higher than that at the upper steps of the wall. It is inferred that this is a result of the larger cross-sectional area lower on the wall, in addition to the greater constriction applied to the lower part by the ground. This restrained the concrete body from expanding, thus restricting crack generation (Fig.6). This effect is also indicated in the relationship between strength and modulus of static elasticity of cores (Fig.8).

It is clear that the inferred effects of temperature and humidity on the strength of ASR-deteriorated concrete are in accord with the results of strength tests carried out using a Schmidt rebound hammer.

4. PREDICTION OF PROGRESS OF DETERIORATION IN ASR-DAMAGED CONCRETE

4.1 Residual Expansion of Concrete Cores

Residual expansions for concrete cores 96 mm in diameter obtained from the retaining walls were measured (Table3 and others). The cores were cut into lengths of 130-250mm or so, and stored in sealed containers maintained at 40℃, and 95% RH for 6 months[5]. Residual expansions of the cores taken concrete walls were below 0.02%. The average expansion of cores taken from the rubber weir anchorage was 0.015%. Judging from the criteria in Japan (residual expansion: 0.1%), it is concluded that ASR expansion was almost complete in the retaining walls (Fig.10).

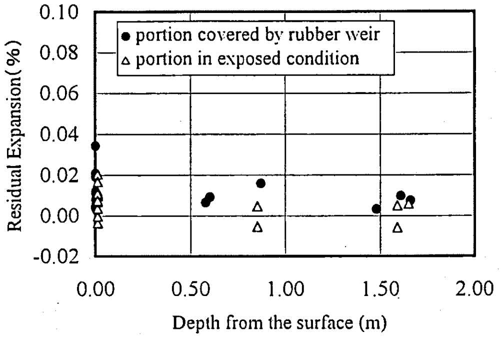

Fig.10 Residual expansion of cores at various locations

4.2 ASR Reactivity of Aggregate

Coarse and fine aggregate particles were taken from cores drilled from the ASR-affected concrete structure. After classifying these particles, several thin sections were made from them to identify the types of mineral existing in the aggregates. Table4 indicates the type of rock making up the coarse aggregate. Observations of these thin sections using a polarization microscope confirm the presence of reaction rims around the periphery of volcanic rock,

Table 4 Petrographical classification of aggregate from concrete

classification	reactivity	weight (g)	number of particles	percentage by weight (%)	percentage by number (%)	Remarks
Volcanic Rock	◎	1417.2	56	10.6	9.3	contained rims
Rhyolite	◎	1249.8	68	9.4	11.4	contained rims
Hornfels	◎	1080.2	56	8.1	9.3	contained rims
Tuff	△	4849.6	229	36.4	38.2	reactive(possibility)
Tuff breccia	△	1676.9	53	12.6	8.8	reactive(possibility)
Dacite	△	1510.8	74	11.3	12.4	reactive(possibility)
Granite,Diorite,Porphyry	×	1543.7	63	11.6	10.5	
Total		13,328.1	599	100.0	100.0	

rhyolite, and hornfels particles. No petrographic classification of fine aggregates was found by observation of the mortar, but reaction rims were found around the periphery of volcanic rock, rhyolite, and hornfels particles as with the coarse aggregate. The JIS chemical method indicates that all coarse aggregates are innocuous, while the fine aggregates are found to be deleterious. The JIS mortar bar method shows that all mortars expanded by less than 0.03% at 6 months, leading to the conclusion that both fine and coarse aggregates in the ASR-damaged concrete are innocuous.

From the evidence of cores drilled from concrete in which ASR has almost run its course, it appears possible that there are few reactive components present. The JIS mortar bar method also notes that small residual expansions may indicate loss of alkalis from the cores during the test period[6]. To check this, we implemented accelerated tests. As seen in Fig.10, residual expansions of concrete cores from the retaining wall were very small. However, when an accelerated tests in saturated NaCl solution (the Danish method[7]) and in 1N NaOH solution (the NBRI method[8]) were conducted on cores from the walls, as shown in Fig.11, the cores expanded significantly, thus confirming that the aggregates in concretes of the structures still contained reactive components even at 14 years after construction.

4.3 Analysis of Pore Solution of Cement Pastes and Mortars

The pore solution in cement pastes and mortars with water/cement ratios of 0.3, 0.4, 0.5, 0.6, and 0.7 (cement: sand = 1: 2, 0.61% $Na_2Oeq.$) were analyzed. Cylindrical specimens (Φ50 × 100 mm) were cured for 7 days in sealed containers at 20°C. The materials used were cement by company- T (alkali: 0.61% Na_2Oeq) and ISO standard sand. Specimens were placed in high-pressure apparatus for extract pore solution. The extracted solutions were immediately diluted in 100-200 parts of water and the Na^+, K^+, Ca^{2+} ion concentrations were measured by the ICP method and OH^- by titration against hydrochloric acid to the phenolphthalein end point. Table5 indicates that the positive and negative ion concentrations in these pore solutions were well balanced. It can also be seen in Fig.12 and Table5 that, for a particular water/cement ratio, the Na^+, K^+, $Ca^{2+}$and OH^- ion concentrations at 7 days are approximately the same as for cement pastes. As the water/cement ratio increases, the Na^+, K^+, and OH^- ion concentrations decreases, while the Ca^{2+} ion concentration increases. However, even in mortars with a water/cement ratio of 0.7, the OH^- ion concentration is around 300 mmol/l. According to Diamond[9], this is high enough to cause ASR.

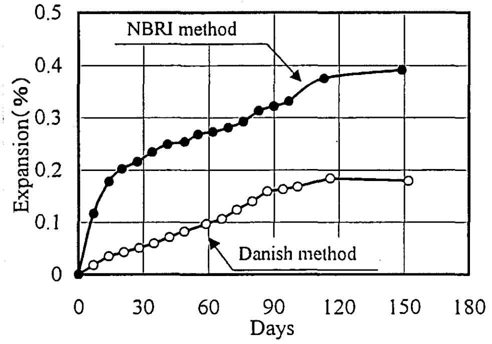

Fig.11 Accelerated testing of concrete cores

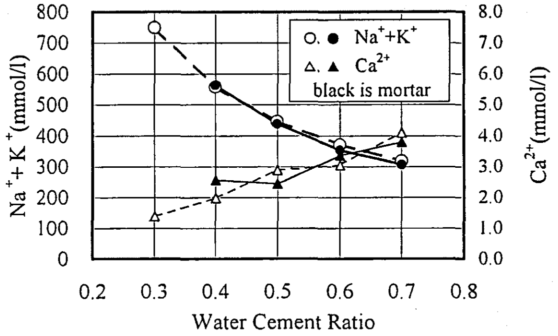

Fig.12 (Na^++K^+) ion concentrations in pore solution

4.4 Evaluation of degree of deterioration from pore solution

In order to develop a method of predicting the future deterioration of ASR-damaged concrete structures, pore solutions extracted from concrete cores were analyzed. These concrete cores were taken from the rubber weir retaining walls (structure A: Table3) as well as from other retaining walls (structure B) located nearby, a concrete snowslide protection barrier (structure C), and the retaining wall of a water tank (structure D).

Structure B is a concrete construction 12m high and from 0.50 to 1.2m wide, and Structure C is a concrete snowslide protection fences (length: 1.3m ; Width: 12.4m; Height: 1.8m). They were built some 38 to 40 years ago, and are not overly exposed to direct sunlight. Structure D is the water tank retaining wall, which is 3.5m high and 0.50 to 1.40m wide and was constructed 23 years ago, is located with a slope to the west. As the hill blocks the sun, there are 2 different conditions in this structure. Exposure to solar radiation of "portion H" is shorter than "portion V". Tables 6 and 7 show the exposure environment of these structures and the mix proportions used for the structures. As the tables show, the water/cement ratios of individual structures were, without exception, approx. 50% to 60%. Table8 (a)-(c) show the results of this analysis. Details are given below.

a) Rubber weir retaining wall (structure A)

Table8 (a)-(c) indicates that the positive and negative ion concentrations in the pore solutions were well balanced. As seen in Fig.13, the $(Na^{+}+K^{+})$ ion concentration at various depths from the surface varies widely. The standard variations in ion concentrations at the surface and the interior are 44.0 and 28.1 mmol/l respectively, so the degree of variation in alkali ion concentration is greater at the surface. This greater variation may be caused by a larger number of cracks around the surface. The intrusion of CO_2 through these cracks causes carbonation of the pore solution, and the fixation[9] of alkalis through the drying process is promoted preferentially in areas along cracks. It is inferred that these various phenomena lead to greater variations in the alkali ion concentration in the surface concrete.

Table5 Ion concentration in cement pastes and mortars

Samples		OH^-	Ca^{2+}	Na^+	K^+	$\Sigma +$	$\Sigma -$
		(mmol/l)					
W/C =0.3	Cement Paste	720.0	1.7	323.8	471.7	798.9	720.0
		708.0	1.2	335.1	451.2	788.8	708.0
		628.0	1.2	272.0	397.2	671.6	628.0
	Mortal	-	-	-	-	-	-
		-	-	-	-	-	-
		-	-	-	-	-	-
W/C =0.4	Cement Paste	550.0	2.3	269.3	330.5	604.4	550.0
		500.0	1.8	236.1	301.7	541.4	500.0
		500.0	1.8	229.3	310.7	543.6	500.0
	Mortal	528.0	2.1	245.2	319.4	568.7	528.0
		464.0	4.5	282.2	303.9	595.1	464.0
		472.0	1.1	251.5	290.8	544.6	472.0
W/C =0.5	Cement Paste	422.0	2.1	225.9	237.8	467.9	422.0
		410.0	3.3	213.1	230.1	449.8	410.0
		400.0	3.3	205.3	225.7	437.6	400.0
	Mortal	388.0	2.4	191.6	219.6	416.0	388.0
		424.0	2.3	228.5	239.9	473.0	424.0
		398.0	2.6	205.5	228.6	439.3	398.0
W/C =0.6	Cement Paste	346.0	3.1	172.8	194.0	372.9	346.0
		352.0	3.1	168.5	194.4	369.0	352.0
		350.0	3.0	181.7	202.8	390.7	350.0
	Mortal	350.0	2.7	167.6	194.6	367.7	350.0
		336.0	3.8	155.4	186.2	349.3	336.0
		328.0	3.6	159.2	196.6	363.0	328.0
W/C =0.7	Cement Paste	318.0	4.5	158.0	163.2	330.3	318.0
		308.0	4.1	158.2	159.7	326.2	308.0
		310.0	3.6	155.6	161.1	324.0	309.0
	Mortal	300.0	3.7	153.1	159.1	319.6	300.0
		292.0	4.3	142.5	153.1	304.1	292.0
		300.0	3.4	151.1	157.8	315.7	300.0

Table6 Exposure environment and W/C ratio of concrete

Structure	Front	Rear	Sunshine	Age (years)	W/C
A	Open	Filled with soil	not good	14	0.59
B	Open	Open	not good	38-40	—
C	Open	Filled with soil	normal	38-40	—
D(valley)	Open	Filled with soil	very good	23	0.54
D(hill)	Open	Filled with soil	good	23	0.54

Table7 Mix proportion of structures

	Gmax (mm)	Sl (cm)	W/C (%)	Air (%)	s/a (%)	(kg/m^3)			
						W	C	S	G
A	40	12	59	5.0	41.3	156	265	764	1,101
D	40	8	54	4.0	40.0	152	280	776	1,145

Compared with the alkali ion concentrations in cores taken from other locations, those in cores taken from the locations indicated by dotted circles in Fig.13 are relatively low. These locations are characterized by large numbers of cracks. Since it was confirmed that these fractures did not occur during core drilling, possible causes for the lower ion concentrations in these locations may be leakage of alkalis as a result of rainwater intrusion through these cracks, carbonation of the pore solution as a result of the intrusion of carbon dioxide through the cracks, and the fixation[10] of alkalis through drying adjacent to the cracks. As noted before, positive ion (Σ +) and negative ion (Σ −) concentrations are always balanced in pore solution, so we can consider that the (Σ +) ion concentration of $[Na^{+}]$,$[K^{+}]$,$[Ca^{2+}]$ is approximately the same as the $[OH^{-}]$ ion concentration. As indicated with asterisks(＊) in Table8 (b), ion concentrations in the vicinity of the surface are lower than at depth. This endorses the proposition that alkali ions in the pore solution near the surface of the concrete are fixed as drying takes place[10]. We could not know the alkalis of the cement which was used for this retaining wall of the rubber weir. But compared with the results of pore solution analysis of cement pastes and mortars (Section 4.3), the [Na^+],[K^+],[Ca^{2+}] ion concentrations in the cores are about 1/10. Thus, the low alkali ion concentrations in the core concretes must be explained by the consumption of ions by continuing ASR over the long period of 14 years. It can be inferred, therefore, that the relatively low residual expansions of cores is due to the low OH^- ion concentrations in the pore solution, because the presence of reactive components is proved by the considerable expansion of the cores in 1N NaOH solutions at 80°C (Fig. 10).

b) Retaining wall (structure B), snowslide protection barrier (structure C), retaining wall of water tank (structure D)

The OH^- ion concentration in pore solutions extracted from cores taken from structures B, C, and D is approximately 51-63 mmol/l on average, lower than in pore solutions taken from structure A. The differences in alkali ion concentration between these structures can be explained by the fact that structures B, C and D are 38–40 years old, so ASR has progressed further as alkalis leached from the concrete by rainwater. Concerning structure D, it is seen that the OH^- ion concentration in pore solutions from "portion V" (38 mmol/l) is smaller than that from "portion H" (92 mmol/l), which was subjected to more significant effects of solar radiation (Table8 (c)). The OH^- ion concentration in a saturated solution of calcium hydroxide at 20°C is 42 mmol/l. The OH^- ion concentrations in the pore solutions of these ASR-affected concrete samples exceed this value.

4.5 Possibility of predicting progress of ASR damage in concrete structures

The findings of this investigation lead to the conclusion that the minimal residual expansion of concrete cores (at 40°C and more than 95% R.H.) with some residual reactive components are due to the reduction in OH^- ion concentration caused by progress of ASR. A threshold OH^- ion concentration of 250 mmol/l for ASR has been proposed[8]. The results of this study do not contradict this figure.

Generally speaking, the progress of ASR deterioration in a concrete structure is determined by the existence or otherwise of reactive components in the aggregates, and whether the OH^- ion concentration in the pore solution exceeds the threshold for ASR. In order to evaluate these criteria, we can use, for example the NBRI test[11], which is an accelerated test for determination of the existence of reactive components. There have been several proposals[12] for the threshold of the test period and the expansion rate of cores, and here we adopt 14 days and 0.01% for the expansion rate. As the threshold of OH^- ion concentration, we use the value of 250mmol/l as proposed[8].

Using the accelerated test and the thresholds described above, we can predict the progress of deterioration in the manner described in Table9. In these criteria, the "B" presupposes that the fall in concentration of OH^- ions is the major criterion for prediction. However it has been found in these examinations that the OH^- ion concentration in concrete cores taken from the surfaces varies greatly due to cracking, etc. So for evaluation of the OH^- ion concentration, the variation must be taken into consideration. Though ASR deterioration is influenced by local environmental conditions, as described in Section 3, where maintenance is concerned, if ASR progresses at any point in a structure, its functionality is usually damaged.

Table8(a) Result of pore solution analysis of structure A(inner side)

core No.		location (m)	OH^-	Ca^{2+}	Na^+	K^+	Σ +	Σ -
			(mmol/l)					
Left Bank	⑥-1	0.52-0.66	70.0	5.0	45.1	24.5	79.6	70.0
	⑥-2	1.00-1.10	104.0	5.1	72.5	40.8	123.5	104.0
	⑥-3	1.10-1.19	80.0	3.6	63.8	32.0	102.9	80.0
	⑥-4	1.54-1.61	110.0	3.8	70.8	44.2	122.4	110.0
	⑥-5	1.95-2.08	120.0	4.6	83.7	49.2	142.0	120.0
	⑥-6	1.95-2.08	98.0	3.8	68.0	37.6	113.2	98.0
	Average		97.0	4.3	67.3	38.0	—	—
Right Bank	①-1	0.00-0.10	122.0	2.1	74.9	51.8	131.1	122.0
	①-3	1.05-1.20	108.0	5.5	67.1	46.7	124.8	108.0
	①-4	1.38-1.48	140.0	1.8	86.7	62.9	153.1	140.0
	①-5	1.93-2.03	64.0	1.0	38.5	28.4	68.8	64.0
	②-1	0.30-0.36	92.0	1.4	51.6	44.5	98.8	92.0
	②-2	0.70-0.87	124.0	2.5	75.9	52.6	133.4	124.0
	②-3	1.20-1.30	98.0	3.9	58.7	39.5	105.9	98.0
	②-4	1.89-1.95	116.0	0.7	64.0	46.6	112.0	116.0
	③-1	0.47-0.58	72.0	9.2	39.6	26.5	84.4	72.0
	③-2	0.85-0.95	134.0	4.7	83.9	57.4	150.6	134.0
	④-1	0.56-0.65	84.0	3.7	64.0	32.0	103.4	84.0
	④-2	1.15-1.27	128.0	2.5	98.4	53.3	156.5	128.0
	④-3	1.76-1.87	142.0	2.5	88.7	63.0	156.6	142.0
	⑤-1	0.33-0.42	126.0	2.7	81.8	57.5	144.6	126.0
	⑤-2	0.78-0.89	136.0	5.2	90.4	53.4	154.2	136.0
	⑤-3	1.27-1.37	132.0	3.1	88.1	59.0	153.3	132.0
	⑤-4	1.49-1.59	160.0	3.9	98.2	66.8	172.9	160.0
	⑤-5	1.83-1.95	120.0	2.9	76.6	51.4	133.7	120.0
	Average		116.6	3.3	73.7	49.6	—	—
Average			111.7	3.5	72.1	46.7	—	—

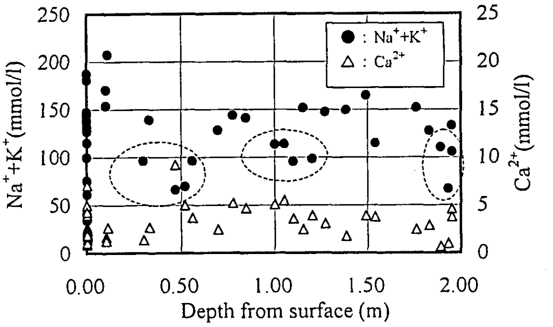

Fig.13 Relations between alkali concentration and depth from surface

Table8(b) Result of pore solution analysis of structure A(surface)

core No.		location (m)	OH^-	Ca^{2+}	Na^+	K^+	Σ+	Σ−	Remarks
			(mmol/l)						
Left Bank	R-1	0.00-0.10	120.0	4.0	77.2	50.4	135.5	120.0	rubber
	R-2	0.00-0.10	104.0	2.7	78.8	49.9	134.2	104.0	
	R-3	0.00-0.10	166.0	2.0	115.1	72.3	191.4	166.0	
	Average		130.0	2.9	90.4	57.5	—	—	
	O-1	0.00-0.08	90.0	1.5	62.2	38.0	103.1	90.0	open
	O-2	0.00-0.06	158.0	0.9	106.2	74.6	182.7	158.0	
	O-3	0.00-0.06	48.0	7.1	21.7	12.6	48.5	48.0	
	Average		98.7	3.2	63.4	41.7	—	—	
Right Bank	R-1	0.00-0.10	150.0	3.9	69.6	74.7	152.1	150.0	rubber
	R-2	0.00-0.10	134.0	5.0	78.6	59.3	147.9	134.0	
	R-3	0.00-0.10	65.7	0.9	42.4	32.7	76.9	65.7	
	R-4	0.00-0.10	72.0	2.5	42.0	33.7	80.7	72.0	
	R-5	0.00-0.08	44.0	2.4	21.5	19.2	45.5	44.0	
	R-6	0.00-0.08	82.0	2.3	55.5	72.2	132.3	82.0	
	R-7	0.00-0.10	94.0	1.8	64.4	50.7	118.8	94.0	
	Average		91.7	2.7	53.4	48.9	—	—	
	O-1	0.00-0.10	128.0	2.4	84.7	54.6	144.2	128.0	* Open
	〃	0.10-0.21	150.0	1.7	93.6	60.1	157.1	150.0	
	O-2	0.00-0.11	132.0	4.0	79.3	52.1	139.4	132.0	*
	〃	0.11-0.21	192.0	2.7	116.0	91.3	212.7	192.0	
	O-3	0.00-0.10	118.0	4.3	81.7	51.0	141.2	118.0	*
	〃	0.10-0.18	150.0	1.3	102.2	68.4	173.2	150.0	
	O-4	0.00-0.09	60.0	1.1	33.7	27.5	63.4	60.0	
	O-5	0.00-0.09	110.0	1.9	86.3	61.0	151.1	110.0	
	Average		130.0	2.4	84.7	58.2	—	—	
Average			112.7	2.7	72.0	52.7	—	—	

Table8(c) Result of pore solution analysis of structure B,C,D

core No. (structure)		location (m)	OH^-	Ca^{2+}	Na^+	K^+	Σ+	Σ−	Remarks
			(mmol/l)						
B	①-1	0.00-0.10	62.5	1.2	50.4	15.4	68.3	62.5	
	①-2	0.00-0.10	24.0	2.7	12.1	4.6	22.1	24.0	
	①-3	0.00-0.11	80.0	1.7	60.8	24.9	89.1	80.0	
	②-1	0.00-0.06	56.0	0.6	40.4	17.2	58.9	56.0	
	②-2	0.00-0.07	58.0	1.0	41.4	19.1	62.5	58.0	
	②-3	0.00-0.07	50.0	0.8	34.4	14.7	50.7	50.0	
	②-4	0.00-0.06	66.0	0.8	43.3	16.8	61.6	66.0	
	②-5	0.00-0.04	32.0	0.9	30.3	10.4	42.5	32.0	
	③-1	0.00-0.08	30.0	0.5	21.3	7.5	29.8	30.0	
	③-2	0.00-0.13	68.0	0.3	64.7	18.2	83.7	68.0	
	④-1	0.00-0.10	62.0	1.7	49.5	19.5	72.2	62.0	
	④-2	0.00-0.13	38.0	1.0	32.6	12.4	46.9	38.0	
	⑤-1	0.00-0.09	46.0	5.9	22.2	10.5	44.5	46.0	
	⑤-2	0.00-0.08	48.0	3.0	30.0	15.0	50.9	48.0	
	Average		51.5	1.6	38.1	14.7	—	—	
C	⑥-1	0.00-0.10	110.0	1.2	88.8	33.2	124.4	110.0	
	⑥-2	0.00-0.10	50.0	3.2	35.3	16.7	58.3	50.0	
	⑦-1	0.00-0.10	40.0	4.8	23.2	10.4	43.2	40.0	
	⑦-2	0.00-0.04	40.0	2.0	32.1	16.9	53.0	40.0	
	⑦-3	0.00-0.06	56.0	2.5	35.0	17.6	57.6	56.0	
	⑧-1	0.00-0.08	70.0	1.8	55.8	25.6	85.0	70.0	
	⑧-2	0.00-0.08	40.0	2.1	27.7	15.9	47.7	40.0	
	⑨-1	0.00-0.10	50.0	2.3	41.9	16.4	62.9	50.0	
	⑩-1	0.00-0.07	48.0	1.9	26.7	16.5	47.1	48.0	
	⑩-2	0.00-0.10	80.0	0.3	55.1	38.7	94.5	80.0	
	⑪-1	0.00-0.05	60.0	3.5	38.0	16.5	61.6	60.0	
	⑪-2	0.00-0.08	16.0	0.7	8.4	2.9	12.6	16.0	
	⑬-2	0.00-0.10	122.0	1.5	86.8	44.1	134.0	122.0	
	⑬-3	0.00-0.10	100.0	0.9	68.0	38.1	107.8	100.0	
	Average		63.0	2.1	44.5	22.1	—	—	
D	H-1	0.15-0.27	42.0	3.8	22.2	8.8	38.7	42.0	Portion H
	H-2	0.12-0.27	124.0	2.3	96.5	29.0	130.1	124.0	
	H-3	0.12-0.27	110.0	2.2	81.5	20.0	106.0	110.0	
	Average		92.0	2.8	66.7	19.3	—	—	
	V-1	0.12-0.26	52.0	3.7	29.9	8.9	46.3	52.0	Portion V
	V-2	0.13-0.27	30.0	4.1	16.7	5.3	30.1	30.0	
	V-3	0.11-0.24	32.0	6.2	13.7	5.4	31.4	32.0	
Average			38.0	4.7	20.1	6.5	—	—	

Table9 Criteria for determining possibility of ASR progress in future

		OH$^-$ ion concentration	
		≧ 250 (mmol/l)	≦ 250 (mmol/l)
Expansion in NBRI test (14days)	≧ 0.1%	A	B
	≦ 0.1%	C	D

Note:

A: high possibility because of high OH$^-$ ion concentration and expansion
B: little possibility because of low OH$^-$ ion concentration (※)
C: little possibility because of low expansion
D: little possibility because of low OH$^-$ ion concentration and expansion
※ In the evaluation of OH$^-$ ion concentration, variations from place to place must be taken into consideration.

Thus we do not take environmental conditions into consideration.

It will now be necessary to verify the threshold proposed in this study and brush up these criteria. This will be a future work.

5. CONCRUSION

In this study, we have investigated concrete structures under natural conditions in order to evaluate the effect of environment on the degree of ASR damage, and to analyze concrete pore solutions with the aim of predicting progress of ASR deterioration. The results obtained in this study are summarized as follows:

(1) Concrete exposed to high temperature and humidity exhibits signs of deterioration caused primarily by ASR, and the crack density in such concrete is high while the strength of cores is low. In contrast, concrete protected from isolation and water ingress has a lower crack density and retains a higher strength.

(2) It is inferred that cracks caused by freezing-thawing cycles play a significant role in the progress of ASR deterioration. It is assumed that deterioration is promoted by the combination with other factors.

(3) Analysis of the pore solution in cement pastes and mortars with water/cement ratios of 0.3, 0.4, 0.5, 0.6, and 0.7 showed that, for a particular water/cement ratio, the Na$^+$, K$^+$, Ca^{2+}, and OH$^-$ ion concentrations are approximately the same in mortar and cement paste. As the water/cement ratio increases, the Na$^+$, K$^+$, and OH$^-$ ion concentrations decrease while Ca^{2+} ion increases.

(4) Compared with the initial conditions, the levels of Na$^+$, K$^+$, Ca^{2+}, and OH$^-$ ions in concrete damaged by ASR are about 1/10. The low alkali ion concentrations of such concrete can be explained by the consumption of ions by ASR as it progresses over a long period.

(5) The degree of variation in alkali ion concentration is greater at the surface because of carbonation caused by the intrusion of CO_2 through many cracks and the fixation of alkalis through the drying process. Further the OH$^-$ ion concentration in pore solution from concrete subjected to more significant effects of solar radiation is smaller, accelerating ASR deterioration.

(6) We propose criteria for determining the possibility of future progress of ASR. This criteria is based on the fact that ASR is a chemical reaction between reactive components in the aggregates and alkalis in the pore solution. The criteria are applied by means of the NBRI test, which is used to judge whether concrete cores contain reactive components or not, and the OH$^-$ ion concentration in the pore solution of concrete cores. A future task is to verify the threshold values proposed in this study and brush up the criteria.

References

[1] Takeuchi,K., Kawamura,M., Torii,K., and Tanikawa,S: Expansion and Cracking due to the Alkali-Silica Reaction in Concretes under Natural Environments, Concrete Research and Technology, Vol.6, No.1, pp.11-19, Jan.1995

[2] Barneyback , R.S., and Diamond, S.: Expression and Analyses of Pore Fluids from Hardened Cement Paste Mortars, Cement and Concrete Research, Vol.11,No.2, pp.279-285, 1981

[3] Kawamura,M., Takeuchi,K., and Sugiyama,A: Mechanisms of the Influence of NaCl Externally Supplied on the Expansion of Mortars due to the Alkali-Silica Reaction, Proc. of JSCE.,No.502/V-25, pp.93-102, 1994

[4] The Society of Materials Science Japan, 1985. "The Symposium of Alkali-Silica Reaction" , pp. 29-41

[5] Japan Concrete Institute, The State of Art of Technology on Durability Diagnosis, Report of Durability Diagnosis Committee, 1989 (in Japanese)

[6] Kawamura,M., Some Problems on Durability of Concrete Structure and their Preventive Measures; Alkali-Aggregate Reaction-No.2, Concrete Journal, Vol.11,No.5, pp.68-75, 1994 (in Japanese)

[7] Chatterji,S.: An Accelerated Method for the Detection of Alkali-Aggregate Reactivities of Aggregate, Cement and Concrete Research ,Vol.8,No.5, pp.647-649,1978

[8] Oberholster,R.E., and Davies, G.: An Accelerated Method for Testing the Potential Alkali Reactivity of Siliceous Aggregates, Cement and Concrete Research, Vol.16, pp. 181-189, 1986

[9] Diamond, S.: Alkali Reactions in Concrete-Pore Solution Effects, Proc. 6th Intl. Conf. Alkalis in Concrete, Copenhagen, pp.155-166, 1983

[10] Diamond, S. : Alkali Silica Reaction-Some Paradoxes, Proc.of the 10th Intl. Conf. on AAR in Concr., Melbourne, pp.3-14,1996

[11] ACI: States-of-the-Art on Alkali-Aggregate Reactivity, ACI 221.1R-98, pp18-19,1998

[12] Grattan-Bellew, P.E .: A Critical Review of Accelerated ASR Test, Proc. 10th Intl. Conf. on AAR in Concr., Melbourne, pp. 27-38, 1998